AXISYMMETRIC ANALYSIS OF INTERNALLY PRESSURIZED ROTATING CYLINDER USING FEM UNDER THERMAL ENVIRONMENT

A project report submitted to the ***National Institute of Technology Rourkela*** *in partial fulfillment of the requirements Of the* ***M. Tech Dual Degree*** *in*

Mechanical Engineering

By

Adarsh Ranjan Padhy

(Roll Number: 711ME4078)

under the supervision of

Prof. R. K. Behera

May, 2016

Department of Mechanical Engineering

National Institute of Technology Rourkela

Mechanical Engineering
National Institute of Technology Rourkela

May 24, 2016

Certificate of Examination

Roll Number: 711ME4078

Name: Adarsh Ranjan Padhy

Title of Dissertation: Axisymmetric analysis of internally pressurized rotating cylinder using FEM under thermal environment

I the below signed, after checking the project report mentioned above and the official record book of the student, hereby state my approval of the project report submitted in partial fulfillment of the requirements of the M. Tech Dual Degree in Mechanical Engineering at National Institute of Technology Rourkela. I am satisfied with the volume, quality, correctness, and originality of the work.

Date:

Prof. R. K. Behera
Dept. of Mechanical Engineering
National Institute of Technology
Rourkela - 769008

Mechanical Engineering
National Institute of Technology Rourkela

Prof. Rabindra Kumar Behera

Associate Professor,
Machine Design & Analysis,
NIT Rourkela

May 24, 2016

Supervisor's Certificate

This is to certify that the work presented in this dissertation entitled "*Axisymmetric analysis of internally pressurized rotating cylinder using FEM under thermal environment'*" by "*Adarsh Ranjan Padhy*", Roll Number 711ME4078, is a record of original research carried out by him under my supervision and guidance in partial fulfillment of the requirements of the *M. Tech Dual Degree* in *Mechanical Engineering*. Neither this dissertation nor any part of it has been submitted for any degree or diploma to any institute or university in India or abroad.

Prof. R. K. Behera

Principal Supervisor

Declaration of Originality

I, *Adarsh Ranjan Padhy*, Roll Number *711ME4078* hereby declare that this thesis entitled "*Axisymmetric analysis of internally pressurized rotating cylinder using FEM under thermal environment*" represents my unique work carried out as a post graduate student of NIT Rourkela and, to the best of my awareness, it encompasses no material formerly published or penned by another person, nor any information presented for the award of any other degree or diploma of NIT Rourkela or any other institution. Any involvement made to this research by others, with whom I have worked at NIT Rourkela or elsewhere, is overtly acknowledged in the project report. Works of other authors cited in this thesis have been duly acknowledged under the section "Bibliography". I have also submitted my original research records to the scrutiny committee for evaluation of my project report.

I am fully aware that in case of any non-compliance detected in future, the Senate of NIT Rourkela may withdraw the degree awarded to me on the basis of the present dissertation.

May 24, 2016

NIT Rourkela

Adarsh Ranjan Padhy

Acknowledgment

I place on record and warmly acknowledge the continuous encouragement, helpful supervision, well-timed suggestions and stirred guidance offered by our guide Prof. R. K. Behera, Professor, Department of Mechanical Engineering, National Institute of Technology, Rourkela, in bringing this report to a successful completion. An erudite teacher and a magnificent person I consider myself fortunate to have worked under his supervision.

I would like to express my gratefulness to Prof. S. S. Mahapatra (Head of the Department) and Prof. D. R. K Parhi (Project Coordinator) for their constructive suggestions and encouragements at various phases of the work. I am also thankful to all staff & members of Department of Mechanical Engineering, NIT Rourkela.

Finally I extend my gratefulness to one and all who are directly or indirectly involved in the successful completion of this project work.

May 24, 2016
NIT Rourkela

Adarsh Ranjan Padhy
Roll Number: 711ME4078

Abstract

The work done under this project is based on mathematical approach for analyzing stress of a homogeneous, isotropic, internally pressurized rotating cylinder under thermal conditions. The equations of importance for this analysis have been derived by using the general stress equilibrium, Kirchhoff's law of heat conduction and Newton's law of force equilibrium. The finite element method will be used to find out the stresses and displacements at each node of isoparametric elements (Bilinear). FEM results so obtained will be then compared with the results from analysis using ANSYS.

The reason for doing comparison is to have an idea about the variance in the results of FEM by analytical method from the approximate solution obtained from ANSYS analysis and to see the extent up to which the results of FEM meet the accurate values by increasing the number of elements.

***Keywords*: rotating cylinder; stress analysis; temperature gradient; FEM.**

Contents

List of Figures

List of Tables

Nomenclature

σ_{rr} = radial stress components

$\sigma_{\theta\theta}$ = circumferential stress components

ρ = the density

r = radius of the cylinder

ω = rotational speed of the cylinder

E = the modulus of elasticity density

α = linear expansion coefficient

K = thermal conductivity through the wall thickness

T = temperature of the cylinder wall

h = convective heat transfer coefficient

υ = Poisson's ratio

Chapter 1

Introduction

Stress analysis of pressurized cylinder is essential in engineering considering its widespread application. The research on stress and strain analysis in a cylinder under rotation has never taken a halt because of its ample importance in various fields of engineering & technology. Some of the commonly found structure such as pressure vessels, rocket engines, domes, submarine hulls, cooling towers etc. possess near axisymmetric geometry. If we neglect holes, attachments, and so on irregularities, their geometry can be approximated as perfectly axisymmetric i.e. these are essentially solid of revolution. They are usually made of isotropic materials and are supposed all-round the periphery. Thus the boundary conditions and the material properties can also be approximated as axisymmetric. When subjected to an axisymmetric loading such as internal pressure/ thermal gradient/ centrifugal force, the resulting deformation and stresses are also perfectly axisymmetric.

1.1. Axisymmetric solids:

Analysis of axis-symmetrically loaded structures of revolution under axisymmetric loading comes under the purview of axisymmetric problem. By a creating cross section which rotates a complete revolution about an axis, as shown in figure below, a structure of revolution (SOR) is obtained. Structures obtained in such a way are said to be rotationally symmetric.

The technical importance of SOR is vital for the trailing practical aspects:

1. Manufacture: manufacturing of axisymmetric bodies are comparatively simpler than the bodies with more complicated and asymmetric models. E.g. pipes, rods, axles, cylinders, wheels, buckets, containers, saucer, screws etc.

2. Specific strength: axisymmetric configuration offer added strength/weight ratio for the advantageous allocation of the material, hence more desirable.
3. Multipurpose: hollow axisymmetric components can be used for various purposes, as in containers, cylinders, vessels, tanks, rockets drums, etc.

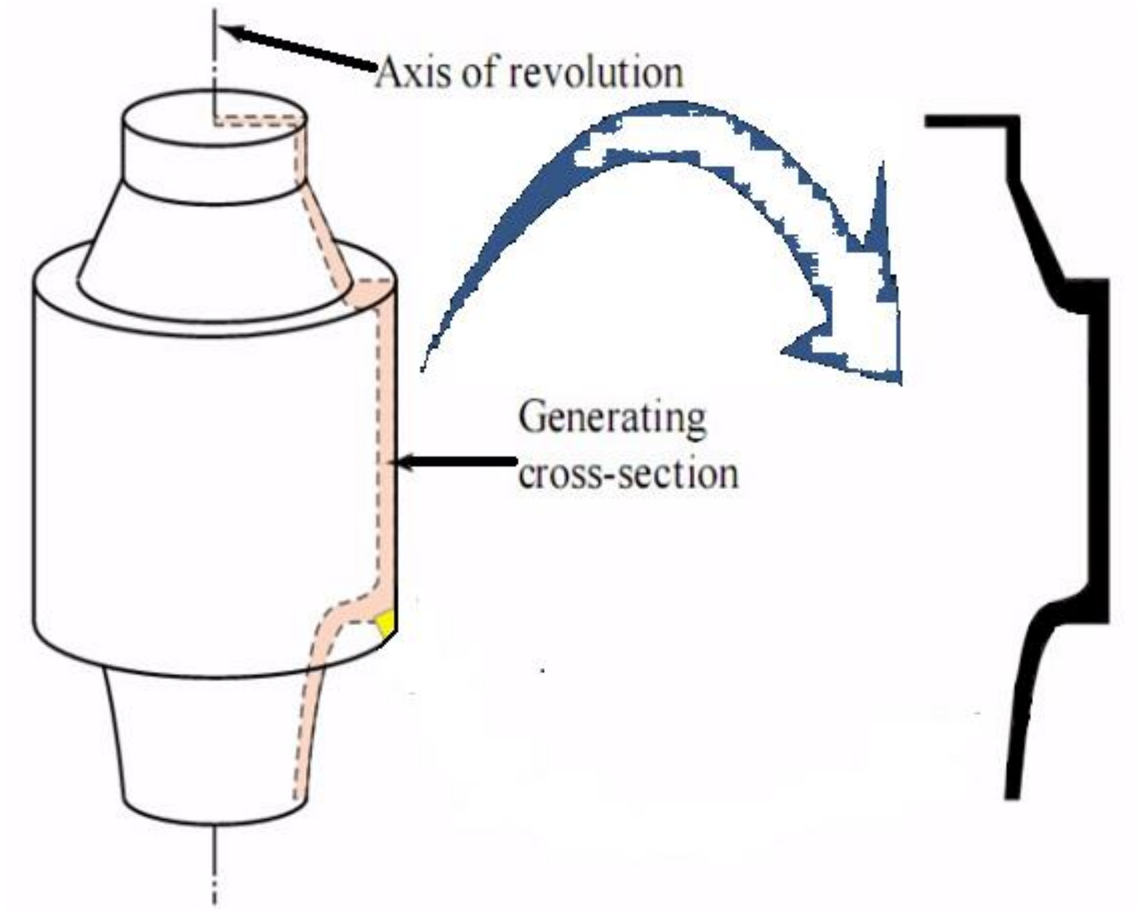

Fig 1: SOR created by circling a cross-section about the axis of rotation

In storage and carriage of fluids, application of SOR i.e. cylinders, vessels, containers and rotating & reciprocating machines (turbines, pumps, shafts, engines etc.) can be found predominantly. But a SOR does not essentially signify an axisymmetric problem. The loading as well as the boundary conditions must be same in angular coordinate. It has been presented in below figure for different loads in different directions

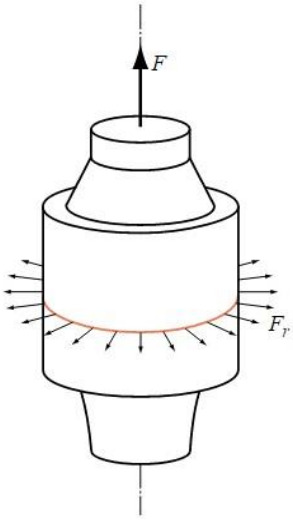

Fig 2: Axisymmetric loading of a SOR:
Fr = radial load, F = longitudinal load

If the conditions

(i) Axisymmetric modeling and (ii) Axisymmetric loading

are encountered, then the axisymmetric response of the structure is obtained. Such structures are also called circumferentially symmetric. By this, it has been indicated that all variables in the analysis i.e. deformations, stresses and strains, are free of the angular coordinate defined later.

1.2. Some SOR Examples:

Structural components of vital importance in general have axisymmetric geometry such as cylinders, but the entire structure is not a SOR. Some of the commonly found structure such as pressure vessels, rocket engines, domes, submarine hulls, cooling towers etc. possess near axisymmetric geometry. If we neglect holes, attachments, and so on irregularities, their geometry can be approximated as perfectly axisymmetric i.e. these are essentially solid of revolution.

1.3. Governing equations:

1.3.1. Co-ordinate systems:

A polar coordinate system is implemented to streamline the primitive equations of a general axisymmetric problem.

Let r = radial distance of the element under consideration z = longitudinal coordinate of the element under consideration

θ = angular coordinate of the element under consideration

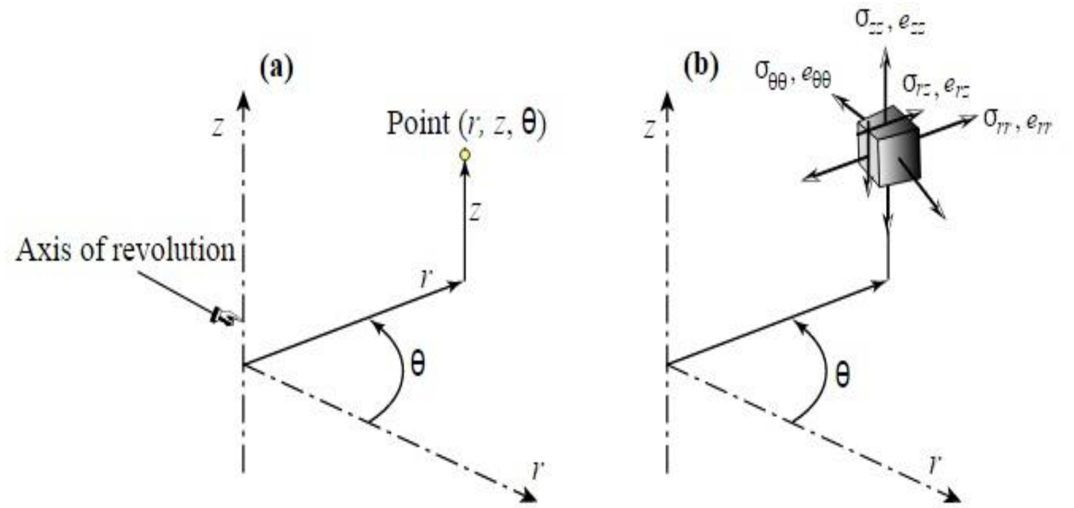

Figure 3: (a) Polar coordinate system (r, z, θ) for analysis of an axisymmetric structure; (b) Stresses and strains with respect to polar coordinate system.

1.3.2. Associated Parameters and general equations:

The polar coordinate system is coordinated along the radial, longitudinal and angular directions respectively. The deformations and the stresses induced in the axisymmetric cylinder are considered to be symmetric.

Hence the equation of equilibrium in the radial direction, neglecting the components of body force, is reduced to the form

$$\sigma'_{rr} + \frac{\sigma_{rr} - \sigma_{\theta\theta}}{r} = -\rho r \omega^2 \dots\dots\dots\dots (1)$$

Where σ_{rr} **is** the radial and $\sigma_{\theta\theta}$ is the hoop stress components; **ρ** is the material density and (') denotes differentiation of variables with respect to r.

The radial strain ε_{rr}, hoop strain $\varepsilon_{\theta\theta}$ and thermal strain ε_t can be written as

$$\varepsilon_{rr} = u'_r \dots\dots\dots\dots (2)$$

$$\varepsilon_{\theta\theta} = \frac{u_r}{r} \dots\dots\dots\dots (3)$$

$$\varepsilon_t = \alpha T \dots\dots\dots\dots (4)$$

Chapter 2

Literature Review

Analyzing stresses in a cylindrical vessel has remained significant in the arena of engineering & technology. Cylindrical vessels have become the focus of research for the recent times owed to its widespread usage in chemical industries, plants, automobiles and submarine hulls. Stress analysis of axisymmetric cylinders subjected to several types of loading has been done by numerous research scholars in isotropic or functionally graded materials.

The elastic stability of adhesive joints under axisymmetric loads is elaborated by [1] Paul E Lyon and it is shown that various parameters affect in various ways to the overall dimensional and structural stability of a cylindrical adhesive joint. Piling order of the composite, the bond span, and the bond width are essentially the key factors in influencing the dimensional stability.

The stress and deformation change along the radial direction of a rotating functionally graded material internally pressurized cylinder subjected is shown by [2] Nejad and Rahimi.

The problem of thick walled conical shells subjected to fluctuating force by second order shear deformation theory is solved by [3] Eipakchi. The computed deformations and stresses are then compared with the FEM solutions and the first order shear deformation theory results.

The equations for obtaining the dislocation and stresses in conical vessel under several axisymmetric loading are also derived by [5] Tavares. Creep analysis of axisymmetric bodies has been completed by many of the researchers.

The extensive formulas for obtaining the stresses in a conical shell are put forward by George [4] Hausenbauer.

The statistic that the creep arises along the favored directions by making an originally isotropic solid anisotropic is found by [6] Taira and Wahl.

Notable contributions to analysis of anisotropy on creep behavior of cylinder are found by [7] Bhatnagar, Arya, pai, etc.

A similar conclusion is made by [8] Renton and Vinson, they stated that redundant overlap length diminishes as the positive stress returns.

Considering large strain to be present, [11] Rimrott had made an analysis on creep of an internally pressurized thick-walled tubes & they showed that the creep rate of a an internally pressurized thick walled cylinder increases, even though the creep rate of the same material when subjected to constant true stress in simple tension remains constant.

In aggregation with [9] Hart-Smith and Renton and Vinson, Kim et al., unrecovered that the overlap length is significant only within a limited range. He stated that with an overlap length-to width ratio of less than one, the failure load increases as overlap length decreases and with an overlap length-to-width ratio greater than one, the failure load vary negligibly.

To study the variation of creep under elevated thermal conditions is studied by [12] Nadai. By decreasing the bond line thickness, a more uniform stress distribution results: it is found by Anderson et al.

In their analysis on adhesive properties, [14] Shimoda et al. found that the adhesive bond strength is sensitive to the bond line thickness at cryogenic temperatures.

The overlap length is critical to joint strength was also recognized by [15] Potter et al. They found that the overlap length essentials to be long enough to transfer the pragmatic load across the joint without facing failure in the middle of the joint. They also observed that the crack propagation distance in the adhesive comes under the effects of the overlap length before reaching a critical crack length.

In their testing of composite linkages for cryogenic uses, [16] Graf et al. found an improved overlap length of 7.62 cm for their test samples. Potter et al. also acknowledged that the overlap length is a critical constraint for analyzing joint strength. It needs to be long enough for transferring the applied load across the joint without experiencing failure in the middle of the joint. They also observed the crack propagation distance in the adhesive before reaching a critical crack length varies with the overlap length.

An examination appropriate for assembling of cylindrical ducts was established by [17] Nemes et al. and [18] Shi and Cheng .

Chapter 3

Methodology

3.1. FEM:

The stresses and strains for any kind of body for whom the particular results has not yet been obtained, can be found by using finite element method. It has nowadays developed to be an essential part of Computer Aided Engineering (CAE). It is now extensively used in the analysis and design of many difficult problems. It began as an augmentation of matrix methods for structural analysis. It was originally identified as a method only for structural analysis but now its application range from structural analysis to thermal to biometrics to electromagnetism and many more.

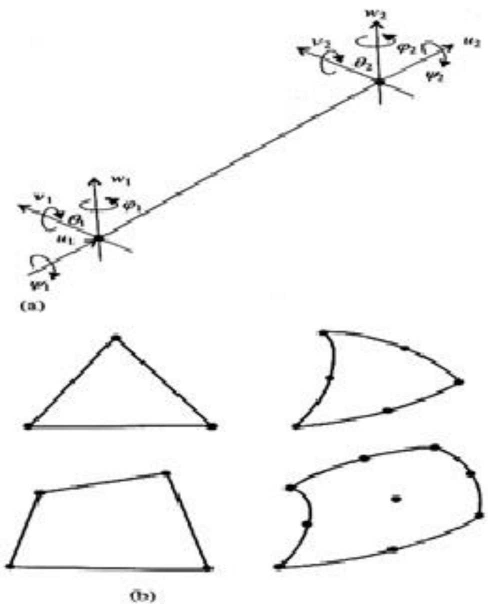

Fig 4: (a) General frame element (Six d.o.f. per node) (b) Common 2-d element

From simple static problems (linear) to highly complex transient dynamics problems (nonlinear) can be accurately solved using the FEM. The field of finite element analysis has improved and now rests on extensive mathematical formulation. Much powerful software is available for analysis using FEM enabling its prevalent use in several industries.

Structural analysis is possibly the very common engineering method in design. The term “structural” not only implies civil works such as buildings & structures, but also mechanical structures such as ships, aircrafts, automobiles and machine housings, as well as machine parts such as bearings, gears & clutches etc. In this project, isoparametric (bilinear) elements will be used for solving the problem.

3.1.1. Isoperimetric element:

A bilinear element with four nodes having two degrees of freedom at each node is shown in the Fig 5.

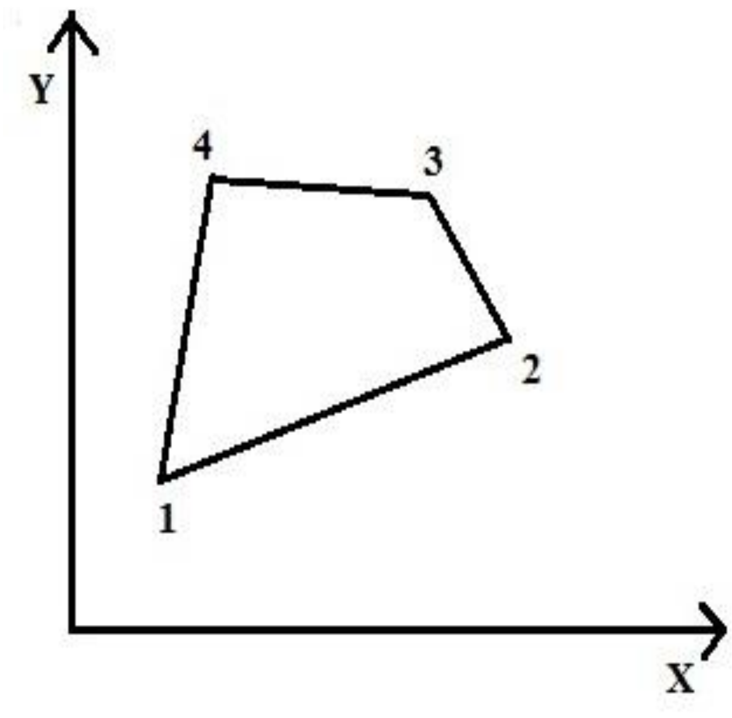

Fig 5: Bilinear Quadrilateral Element with four nodes

By the use of the natural coordinate ξ and η as shown below, the element is now mapped into a rectangle,

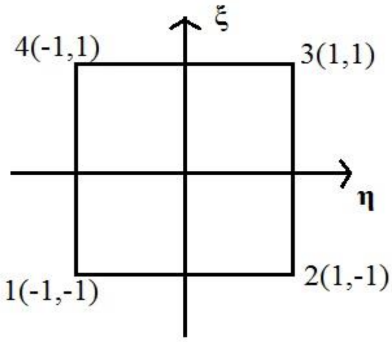

Fig 6: Natural coordinates of a Bilinear Quadrilateral Element

For the 2-element bilinear quadrilateral;

The shape function are

$$N_1 = \frac{(1-\xi)(1-\eta)}{4}$$

$$N_2 = \frac{(1+\xi)(1-\eta)}{4}$$

$$N_3 = \frac{(1+\xi)(1+\eta)}{4}$$

$$N_4 = \frac{(1-\xi)(1+\eta)}{4}$$

For the element under consideration matrix [B] is given by;

$$[B] = [B_1]\,[B_2]\,[B_3]$$

$$[B_1] = \begin{bmatrix} 1 & 0 & 0 & 0 \\ 0 & 0 & 0 & 1 \\ 0 & 1 & 1 & 0 \end{bmatrix}$$

$$[B_2] = \frac{1}{|J|}\begin{bmatrix} J_{22} & -J_{12} & 0 & 0 \\ -J_{21} & J_{11} & 0 & 0 \\ 0 & 0 & J_{22} & -J_{12} \\ 0 & 0 & -J_{21} & J_{11} \end{bmatrix}$$

Where, Jacobian matrix, $[J] = \begin{bmatrix} \frac{\partial x}{\partial \xi} & \frac{\partial y}{\partial \xi} \\ \frac{\partial x}{\partial \eta} & \frac{\partial y}{\partial \eta} \end{bmatrix}$

$$= \begin{bmatrix} \sum \frac{\partial N_i}{\partial \xi} x_i & \sum \frac{\partial N_i}{\partial \xi} y_i \\ \sum \frac{\partial N_i}{\partial \eta} x_i & \sum \frac{\partial N_i}{\partial \eta} y_i \end{bmatrix}$$

$$= \begin{bmatrix} \left(\frac{1-\eta}{4}\right)(x_2 - x_1) + \left(\frac{1+\eta}{4}\right)(x_3 - x_4) & \left(\frac{1-\eta}{4}\right)(y_2 - y_1) + \left(\frac{1+\eta}{4}\right)(y_3 - y_4) \\ \left(\frac{1-\xi}{4}\right)(x_4 - x_1) + \left(\frac{1+\xi}{4}\right)(x_3 - x_2) & \left(\frac{1-\xi}{4}\right)(y_4 - y_1) + \left(\frac{1+\xi}{4}\right)(y_3 - y_2) \end{bmatrix}$$

$$[B_3] = \begin{bmatrix} \frac{\partial N_1}{\partial \xi} & 0 & \frac{\partial N_2}{\partial \xi} & 0 & \frac{\partial N_3}{\partial \xi} & 0 & \frac{\partial N_4}{\partial \xi} & 0 \\ \frac{\partial N_1}{\partial \eta} & 0 & \frac{\partial N_2}{\partial \eta} & 0 & \frac{\partial N_3}{\partial \eta} & 0 & \frac{\partial N_4}{\partial \eta} & 0 \\ 0 & \frac{\partial N_1}{\partial \xi} & 0 & \frac{\partial N_2}{\partial \xi} & 0 & \frac{\partial N_3}{\partial \xi} & 0 & \frac{\partial N_4}{\partial \xi} \\ 0 & \frac{\partial N_1}{\partial \eta} & 0 & \frac{\partial N_2}{\partial \eta} & 0 & \frac{\partial N_3}{\partial \eta} & 0 & \frac{\partial N_4}{\partial \eta} \end{bmatrix}$$

Where,

$$\frac{\partial N_1}{\partial \xi} = -\left(\frac{1-\eta}{4}\right) \qquad \frac{\partial N_1}{\partial \eta} = -\left(\frac{1-\xi}{4}\right)$$

$$\frac{\partial N_2}{\partial \xi} = +\left(\frac{1-\eta}{4}\right) \qquad \frac{\partial N_2}{\partial \eta} = -\left(\frac{1+\xi}{4}\right)$$

$$\frac{\partial N_3}{\partial \xi} = +\left(\frac{1+\eta}{4}\right) \qquad \frac{\partial N_3}{\partial \eta} = +\left(\frac{1+\xi}{4}\right)$$

$$\frac{\partial N_4}{\partial \xi} = -\left(\frac{1+\eta}{4}\right) \qquad \frac{\partial N_4}{\partial \eta} = +\left(\frac{1-\xi}{4}\right)$$

We have the element stiffness matrix as

$$[K]^e = \int_{-1}^{1}\int_{-1}^{1} [B]^T \, [D][B] \cdot t \cdot |J| \cdot d\xi \cdot d\eta$$

Where, t = thickness of the element considered

Chapter 4

Exact Formulation

Here the equation of equilibrium in the radial direction, neglecting the components of body force, is reduced to

$$\sigma'_{rr} + \frac{\sigma_{rr} - \sigma_{\theta\theta}}{r} = -\rho r \omega^2 \ldots\ldots\ldots\ldots\ldots (1)$$

Where $\boldsymbol{\sigma_{rr}}$ and $\boldsymbol{\sigma_{\theta\theta}}$ are the radial and hoop stress components respectively; $\boldsymbol{\rho}$ is the material density and (') denotes differentiation of variables with respect to r.

For the assumed thick cylinder, $\boldsymbol{\sigma_{rr}}$ and $\boldsymbol{\sigma_{\theta\theta}}$ is written in terms of deformation $\mathbf{u_r}$ by

$$\sigma_{rr} = [C_{11}\varepsilon_{rr} + C_{12}\varepsilon_{\theta\theta} + C_{13}(\alpha T)]E$$

$$\sigma_{\theta\theta} = [C_{12}\varepsilon_{rr} + C_{11}\varepsilon_{\theta\theta} + C_{13}(\alpha T)]E \ldots\ldots (5)$$

Here E(r) is the elastic modulus of the material and C_{11}, C_{12}, C_{13} can be stated in terms of Poisson's ratio 'υ' as:

Plane strain condition:

$C_{11} = (1- \upsilon) / [(1+ \upsilon)(1- 2\upsilon)]$

$C_{12} = \upsilon / [(1+ \upsilon)(1- 2\upsilon)]$

$C_{13} = -1 / (1- 2\upsilon)$

Plane stress condition:

$C_{11} = 1 / (1- \upsilon^2)$

$C_{12} = \upsilon / (1- \upsilon^2)$

C_{13} = -1 / (1- υ)

Substituting the equations (5) into equation (1), we get

$$\frac{d^2u_r}{dr^2}+\left(\frac{1}{E}\frac{dE}{dr}+\frac{1}{r}\right)\frac{du_r}{dr}+\left(\frac{C_{12}}{C_{11}}\frac{1}{Er}\frac{dE}{dr}-\frac{1}{r^2}\right)u_r=-\frac{C_{13}}{C_{11}}\frac{1}{E}\frac{d(E\alpha T)}{dr}-\frac{\rho r\omega 2}{C_{11}E}\ \ldots.(6)$$

The equation (6) is a form of Navier equation in terms of radial deformation.

Here it has been assumed that the material properties are radially constant i.e. the elastic modulus of material 'E', material density 'ρ', coefficient of linear expansion 'α' and the thermal conductivity 'K' through the wall are assumed to be constant.

$$\frac{dE}{dr}=0;\ \frac{d\rho}{dr}=0;\ \frac{d\alpha}{dr}=0;\ \frac{dK}{dr}=0\ \ldots\ldots\ldots\ldots(7)$$

As the variation of Poisson's ratio for engineering materials are relatively small, it is assumed to be constant throughout the material.

From Kirchhoff's law, we know that under steady state heat conduction case, the heat conduction equation for the 1-D problems in polar coordinate simplifies to

$$\frac{\partial}{\partial r}\left(Kr\frac{\partial T}{\partial r}\right)=0\ \ldots\ldots\ldots\ldots\ldots\ldots(8)$$

The thermal boundary condition for the homogeneous hollow cylinder is given by

$$K\frac{dT}{dr}=\ h_a(T-T_a)\ on\ r=a$$

$$K\frac{dT}{dr}=\ h_b(T-T_b)\ on\ r=b$$

Where T_a and T_b are the temperatures on the inner and outer walls of the cylinder, h_a and h_b are the convective coefficients of heat transfer and the subscripts a and b corresponds to radiuses r (a) and r (b), respectively.

The general solution of equation (8) by considering the convective heat transfer coefficient of the material to be constant throughout the material is

$$T=A_1\ln r+\ A_2\ \ldots\ldots\ldots\ldots\ldots\ldots(9)$$

Considering the boundary conditions and the equation (9), we get

$$A_1 = \frac{T_b - T_a}{K\left(\frac{1}{ah_a} + \frac{1}{bh_b}\right) + \ln\left(\frac{b}{a}\right)}$$

$$A_2 = \frac{K\left(\frac{T_b}{ah_a} + \frac{T_a}{bh_b}\right) + T_a \ln b - T_b \ln a}{K\left(\frac{1}{ah_a} + \frac{1}{bh_b}\right) + \ln\left(\frac{b}{a}\right)}$$

By substituting equations (7) & (9) into equations (6), the Navier equation would be,

$$\frac{d^2u_r}{dr^2} + \frac{1}{r}\frac{du_r}{dr} - \frac{1}{r^2}u_r = -\frac{C_{13}}{C_{11}}\alpha\frac{A_1}{r} - \frac{\rho r \omega 2}{C_{11}E}$$

$$r^2\frac{d^2u_r}{dr^2} + r\frac{du_r}{dr} - u_r = -\frac{C_{13}}{C_{11}}\alpha A_1 r - \frac{\rho r \omega 2}{C_{11}E} \dots\dots (10)$$

Equation (10) is the Euler-Cauchy equation (non-homogeneous) whose complete solution is

$$u_r = \left(B_1 + \frac{C_{13}}{C_{11}}\alpha A_1 + \frac{6\rho r \omega 2}{C_{11}}\right) r + B_2 r^{-1} + \frac{\rho r \omega 2}{C_{11}E} r^3 \dots\dots (11)$$

For the hollow cylinder subjected to uniform pressure P on the inner surface, the mechanical boundary conditions can be expressed as

$$\sigma_{rr}|_{r=a} = -P \ , \sigma_{rr}|_{r=b} = 0 \dots\dots\dots\dots (12)$$

Substituting the boundary conditions (12) and equation (11) into equation (3), the constants can be evaluates as

$$B_2 = \frac{\begin{gathered}(3C_{11} + C_{12})\frac{\rho\omega 2}{C_{11}E}(a^2 - b^2) + \\ C_{13}\alpha A_1 \ln\left(\frac{a}{b}\right) + \frac{P}{E}\end{gathered}}{(C_{12} - C_{11})\left(\frac{1}{b^2} - \frac{1}{a^2}\right)}$$

$$B_1 = \frac{(C_{11} + C_{12})\left(\frac{C_{13}}{C_{11}}\alpha A_1 + \frac{\rho\omega 2}{C_{11}E}\right)(a^2 - b^2) + C_{13}\alpha\{A_1(a^2 \ln a - b^2 \ln b) + A_2(a^2 - b^2)\} + \frac{a^2 P}{E} + (3C_{11} + C_{12})\frac{\rho\omega 2}{C_{11}E}(a^4 - b^4)}{(C_{12} + C_{11})(b^2 - a^2)}$$

Chapter 5

Problem Description

4.1. Without thermal load:

For the purpose of validation of the ongoing project procedures, a thin walled cylinder pressure vessel under rotation with the inner radius of a = 1.5 m and the outer radius of b = 1.7 m is taken, which is rotating around the longitudinal at the constant angular velocity of ω = 15 rad/sec. The modulus of elasticity and density of the structural steel, respectively, have values of E = 200 GPa, ρ = 7860 kg/m3. It is also assumed that the Poisson’s ratio, υ, has a constant value of 0.3 or 0.33. The applied internal pressure is 30 MPa.

For the purpose of studying the stress distribution along the cylinder radius, the Von Mises equivalent stress of

$$\boldsymbol{\sigma_{eq}} = \frac{\mathbf{1}}{\sqrt{\mathbf{2}}}[(\boldsymbol{\sigma_{rr}} - \boldsymbol{\sigma_{\theta\theta}})^{\mathbf{2}} + (\boldsymbol{\sigma_{\theta\theta}} - \boldsymbol{\sigma_{z}})^{\mathbf{2}} + (\boldsymbol{\sigma_{z}} - \boldsymbol{\sigma_{rr}})^{\mathbf{2}}]^{\mathbf{0.5}}$$

is plotted in the radial direction for the conditions of plane strain, plane stress and the cylinder with closed ends.

The variation of equivalent stress and radial displacement with angular velocity is shown for plane stress, plane strain, and cylinder with closed ends. These figures suggest that the equivalent stress and radial displacement are significantly affected due to angular velocity.

4.1.1. Element Description:

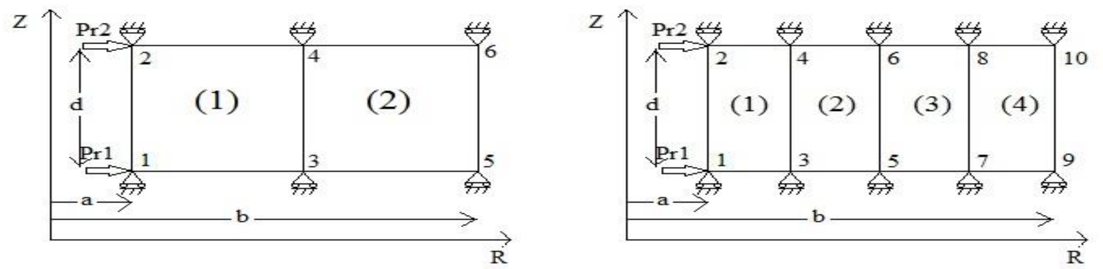

Fig 7: (a) for 2-numbers of elements (b) for 4-numbers of elements

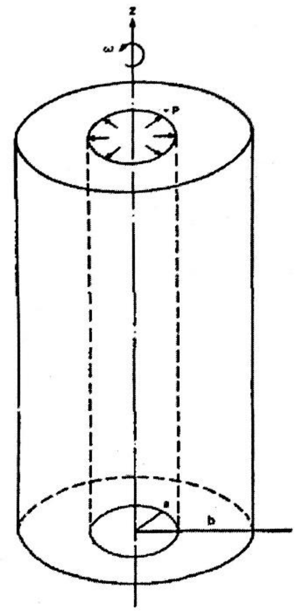

Fig 8: A rotating internally pressurized cylinder

4.2. With Thermal Load:

Taking into account the thermal load, a hollow homogeneous cylinder of inner radius a = 0.5m and the outer radius b = 0.7m, which is rotating around the longitudinal axis at the constant angular speed of ω = 50rad /sec is considered. Here we consider that the surface temperatures at the inner and outer surfaces are described as T_a and T_b respectively. The boundary conditions for temperature are taken as T_a = 10^o C and T_b= 0^o C. The modulus of elasticity, density and thermal coefficient of expansion at the inner radius have the values of E = 200GPa, ρ = $7860 kg/m^3$, α $=12(10)^{-6}/^o$ C, respectively. It is also assumed that the Poisson's ratio υ, has a constant value of 0.3. The applied internal and external pressures are 80MPa and 10MPa respectively.

4.1.1. Element Description:

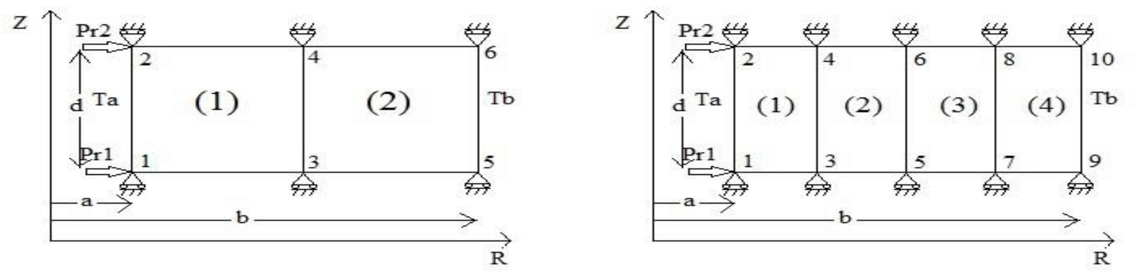

Fig 9: (a) for 2-numbers of elements (b) for 4-numbers of elements

Chapter 6

Results and discussions

5.1. Mathematical Equations:

The mathematical equation for radial displacement has been evaluated by far & the expression for the same is as follows:

$$u_r = \left(B_1 + \frac{C_{13}}{C_{11}}\alpha A_1 + \frac{6\rho r\omega 2}{C_{11}}\right)r + B_2 r^{-1} + \frac{\rho r\omega 2}{C_{11}E}r^3$$

Where,

$$A_1 = \frac{T_b - T_a}{K\left(\frac{1}{ah_a} + \frac{1}{bh_b}\right) + \ln\left(\frac{b}{a}\right)}$$

$$B_1 = \frac{(C_{11} + C_{12})\left(\frac{C_{13}}{C_{11}}\alpha A_1 + \frac{\rho\omega 2}{C_{11}E}\right)(a^2 - b^2) + C_{13}\alpha\{A_1(a^2\ln a - b^2\ln b) + A_2(a^2 - b^2)\} + \frac{a^2P}{E} + (3C_{11} + C_{12})\frac{\rho\omega 2}{C_{11}E}(a^4 - b^4)}{(C_{12} + C_{11})(b^2 - a^2)}$$

$$B_2 = \frac{(3C_{11} + C_{12})\frac{\rho\omega 2}{C_{11}E}(a^2 - b^2) + C_{13}\alpha A_1\ln\left(\frac{a}{b}\right) + \frac{P}{E}}{(C_{12} - C_{11})\left(\frac{1}{b^2} - \frac{1}{a^2}\right)}$$

5.2. Verification through ANSYS:

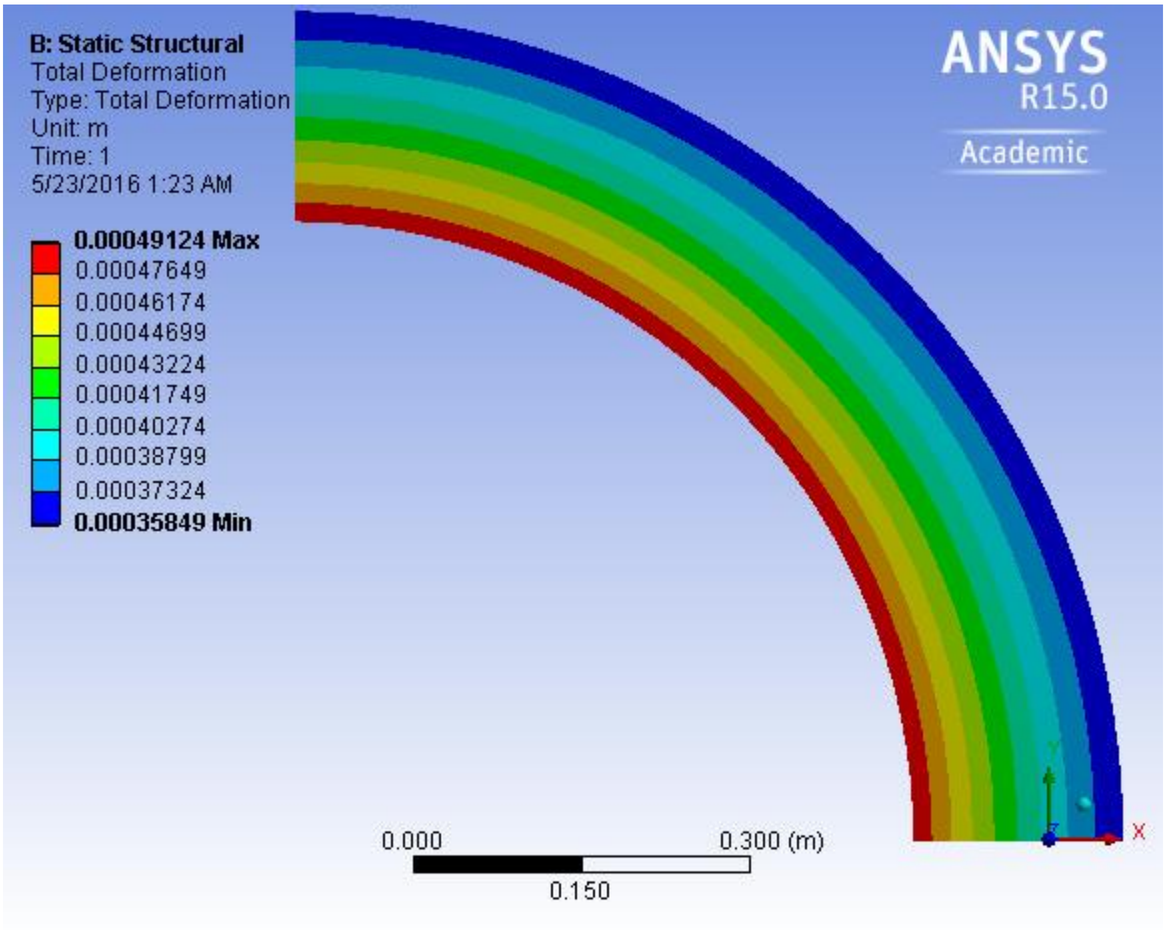

Fig 10: Variation of radial deformation with radial distance for 4 numbers of element

Table 1: Results of ANSYS analysis using 4 numbers of elements

Definition			
Type	Total Deformation	Equivalent (von-Mises) Stress	Radial Stress
Results			
Minimum	3.5849e-004 m	1.5745e+008 Pa	1.5224 e+008 Pa
Maximum	4.9124e-004 m	2.5098e+008 Pa	2.0123 e+008 Pa

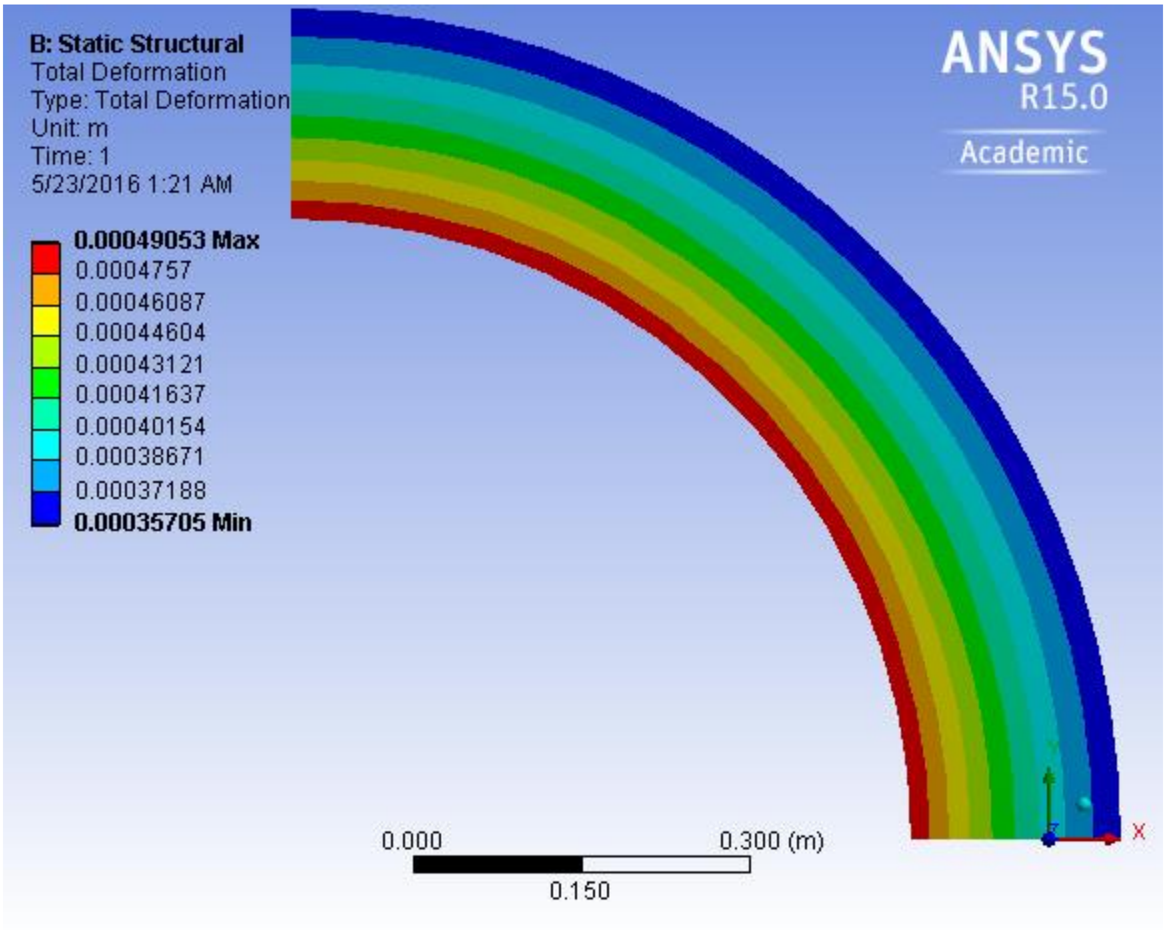

Fig 11: Variation of radial deformation with radial distance for 2 numbers of element

Table 2: Results of ANSYS analysis using 2 numbers of element

Definition			
Type	Total Deformation	Equivalent (von-Mises) Stress	Maximum Principal Stress
Results			
Minimum	3.5742e-004 m	1.5798e+008 Pa	1.4901 e+008 Pa
Maximum	4.9003e-004 m	2.4481e+008 Pa	2.0351 e+008 Pa

5.3. Comparison of results obtained from MATLAB:

Global Stiffness matrix:

For Bilinear Quadrilateral Element
(2-element):

Stiffness matrix, K [12*12] = 1e+07*

1.07	0.65	-0.64	-0.28	-0.01	-0.10	-0.41	-0.25	0	0	0	0
0.65	2.76	-0.10	-2.64	-0.28	0.95	-0.25	-1.07	0	0	0	0
-0.64	-0.10	0.93	-0.25	-0.41	0.47	0.12	-0.11	0	0	0	0
-0.28	-2.64	-0.25	2.72	0.53	-1.07	0.008	0.99	0	0	0	0
-0.01	-0.28	-0.41	0.53	1.80	0.39	-0.94	-0.28	-0.01	-0.10	-0.41	-0.25
-0.10	0.95	0.47	-1.07	0.39	4.33	-0.22	-4.08	-0.28	0.95	-0.25	-1.07
-0.41	-0.25	0.12	0.008	-0.94	-0.22	1.52	0.10	-0.41	0.47	0.12	-0.11
-0.25	-1.07	-0.11	0.99	-0.28	-4.08	0.10	4.25	0.53	-1.07	0.008	0.99
0	0	0	0	-0.01	-0.28	-0.41	0.53	0.73	-0.25	-0.30	0.008
0	0	0	0	-0.10	0.95	0.47	-1.07	-0.25	1.56	-0.11	-1.44
0	0	0	0	-0.41	-0.25	0.12	0.008	-0.30	-0.11	0.59	0.35
0	0	0	0	-0.25	-1.07	-0.11	0.99	0.008	-1.44	0.35	1.52

For Bilinear Quadrilateral Element
(4-element):

Stiffness matrix, K [20*20] = 1e+07*

0.99	0.65	-0.63	-0.28	-0.01	-0.08	-0.41	-0.23	0	0	0	0
0.65	1.27	-0.10	-1.24	-0.28	0.69	-0.25	-0.94	0	0	0	0
-0.63	-0.10	0.96	-0.25	-0.21	0.47	0.11	-0.11	0	0	0	0
-0.28	-1.24	-0.25	1.35	0.51	-0.96	0.008	0.96	0	0	0	0
-0.01	-0.28	-0.21	0.51	1.75	0	-0.85	0	0.82	-0.79	-0.65	0.54
-0.08	0.69	0.47	-0.96	0	2.75	0	0.85	-0.79	0.52	0.57	0.95
-0.41	-0.25	0.11	0.008	-0.85	0	0.79	0	-0.65	0.65	-0.54	0.54
-0.23	-0.94	-0.11	0.96	0	0.85	0	2.58	0.54	0.43	0.65	0.84
0	0	0	0	0.82	-0.79	-0.65	0.54	4.33	0	0.57	0
0	0	0	0	-0.79	0.52	0.65	0.43	0	1.75	0	-0.57
0	0	0	0	-0.65	0.57	-0.54	0.65	0.57	0	1.88	0
0	0	0	0	0.54	0.95	0.54	0.84	0	-0.57	0	2.55
0	0	0	0	0	0	0	0	0.82	-0.79	-0.65	0.54
0	0	0	0	0	0	0	0	-0.79	0.52	0.57	0.95
0	0	0	0	0	0	0	0	-0.65	0.65	-0.54	0.54

0	0	0	0	0	0	0	0
0	0	0	0	0	0	0	0
0	0	0	0	0	0	0	0
0	0	0	0	0	0	0	0
0	0	0	0	0	0	0	0
0	0	0	0	0	0	0	0
0	0	0	0	0	0	0	0
0	0	0	0	0	0	0	0
0.82	-0.79	-0.65	0.54	0	0	0	0
-0.79	0.52	0.65	0.43	0	0	0	0
-0.65	0.57	-0.54	0.65	0	0	0	0
0.54	0.95	0.54	0.84	0	0	0	0
1.72	0.39	-0.94	-0.28	-0.01	-0.10	-0.41	-0.25
0.39	2.93	-0.22	-4.08	-0.28	0.95	-0.25	-1.09
-0.94	-0.22	1.50	0.10	-0.41	0.47	0.12	-0.11
-0.28	-4.08	0.10	3.85	0.53	-1.07	0.008	1.01
-0.01	-0.28	-0.41	0.53	0.74	-0.25	-0.30	0.008
-0.10	0.95	0.47	-1.07	-0.25	1.45	-0.11	-1.49
-0.41	-0.25	0.12	0.008	-0.30	-0.11	0.79	0.35
-0.25	-1.09	-0.11	1.01	0.008	-1.49	0.35	1.49

Table 3: Results using 2 no. of elements in MATLAB using FEM

Definition			
Type	Radial Deformation	Equivalent (von-Mises) Stress	Radial Stress
Results			
Minimum	2.3872e-004 m	1.3901e+008 Pa	1.3556e+008 Pa
Maximum	4.9433e-004 m	2.5112e+008 Pa	2.1344e+008 Pa

Table 4: Results using 4 no. of elements in MATLAB using FEM

Definition			
Type	Radial Deformation	Equivalent (von-Mises) Stress	Radial Stress
Results			
Minimum	2.4841e-004 m	1.4215e+008 Pa	1.3691e+008 Pa
Maximum	4.9554e-004 m	2.5189e+008 Pa	2.1415e+008 Pa

Graphs

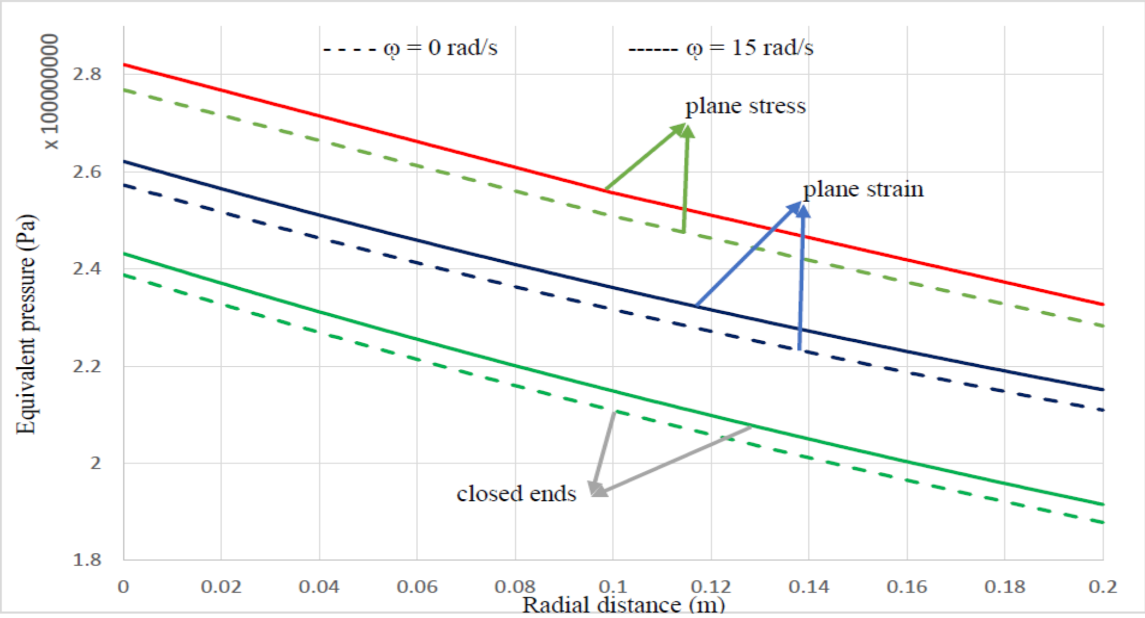

Fig 12: equivalent stress vs radial distance (plane stress, plane strain and cylinder with closed ends)

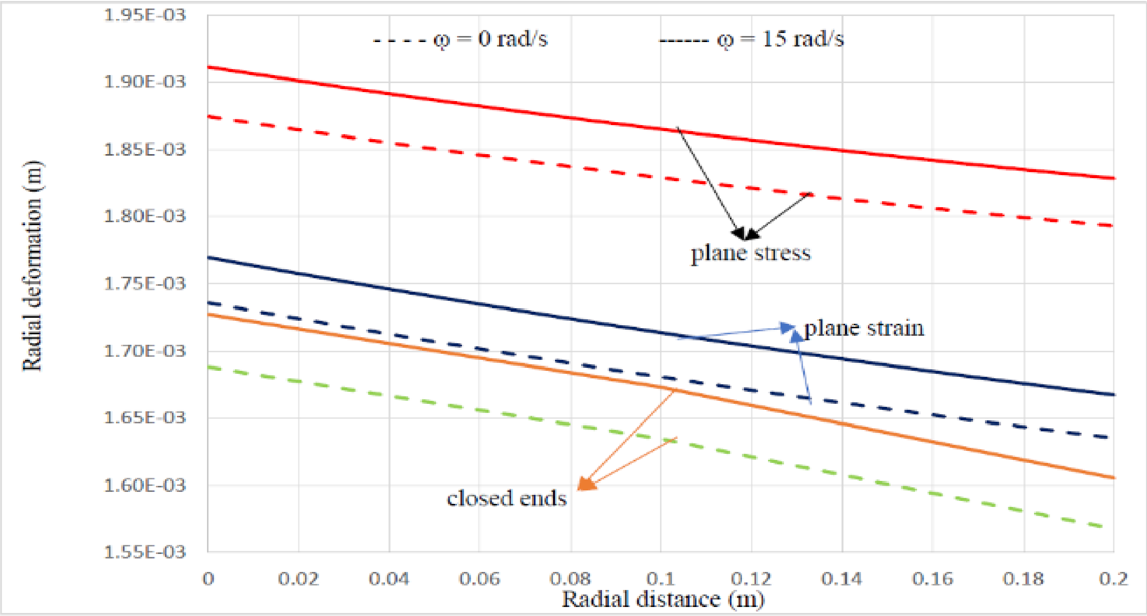

Fig 13: radial displacement vs radial distance (plane stress, plane strain and cylinder with closed end)

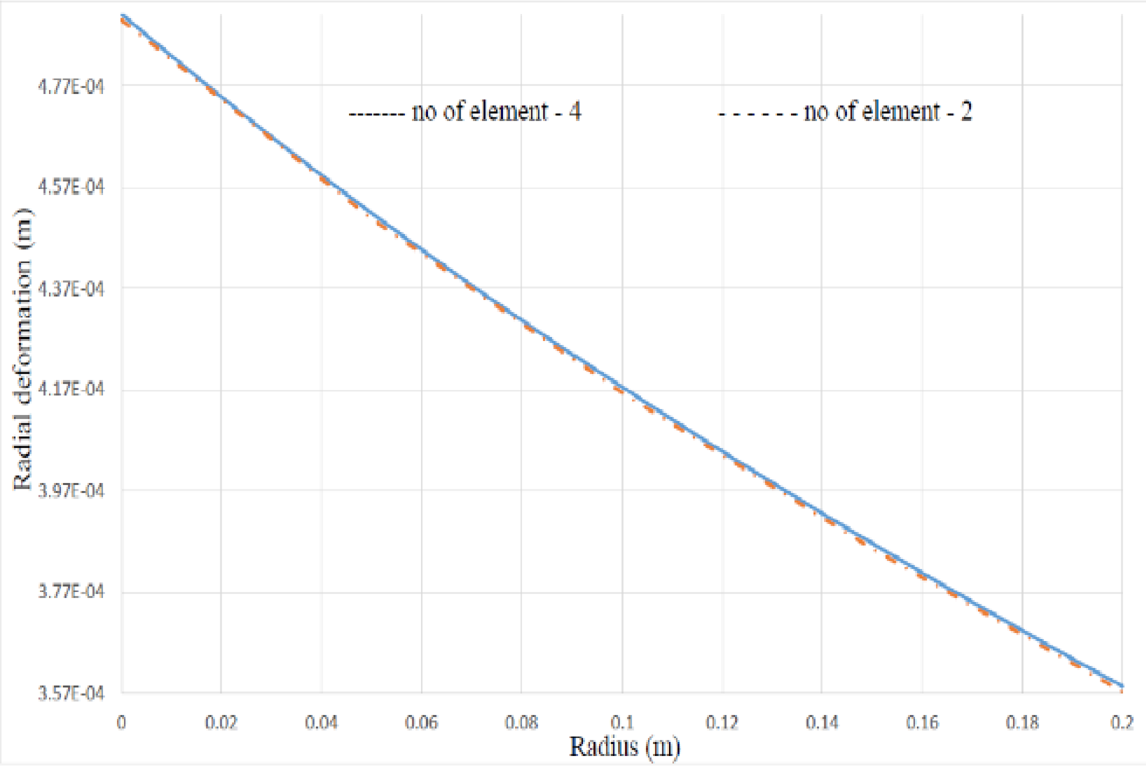

Fig 14: radial displacement vs radius (ω = 50rad /sec).

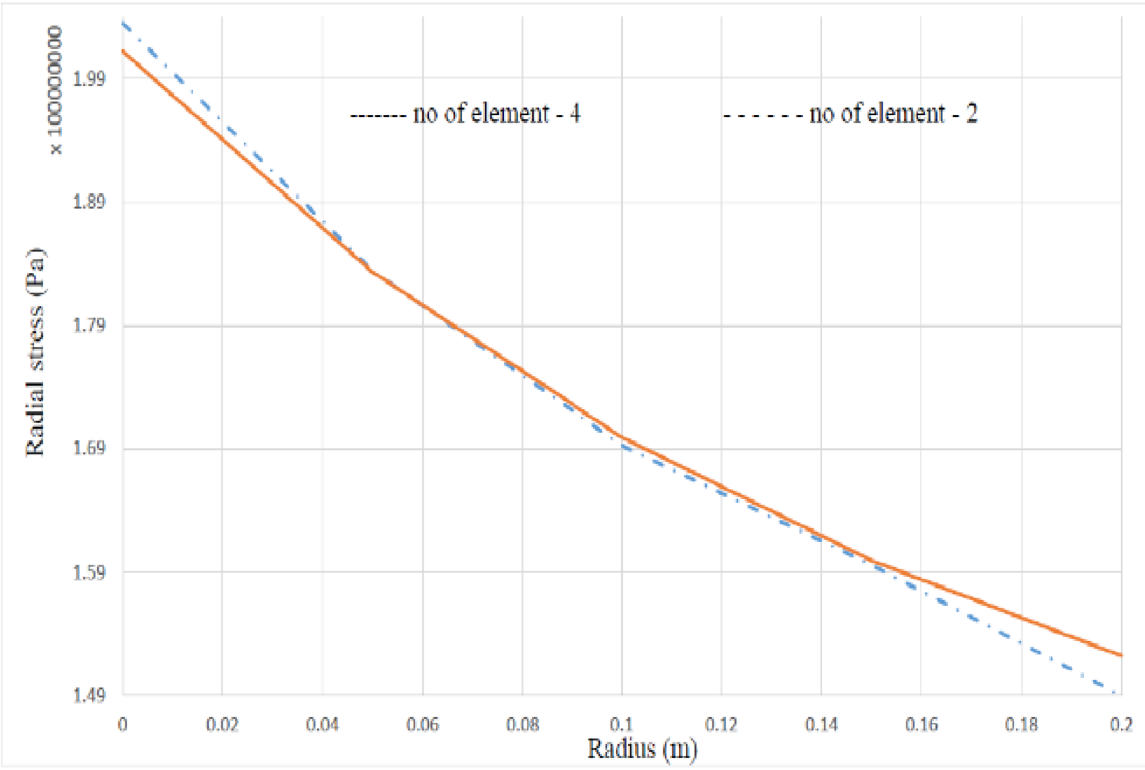

Fig 15: radial stress vs radius (ω = 50rad /sec).

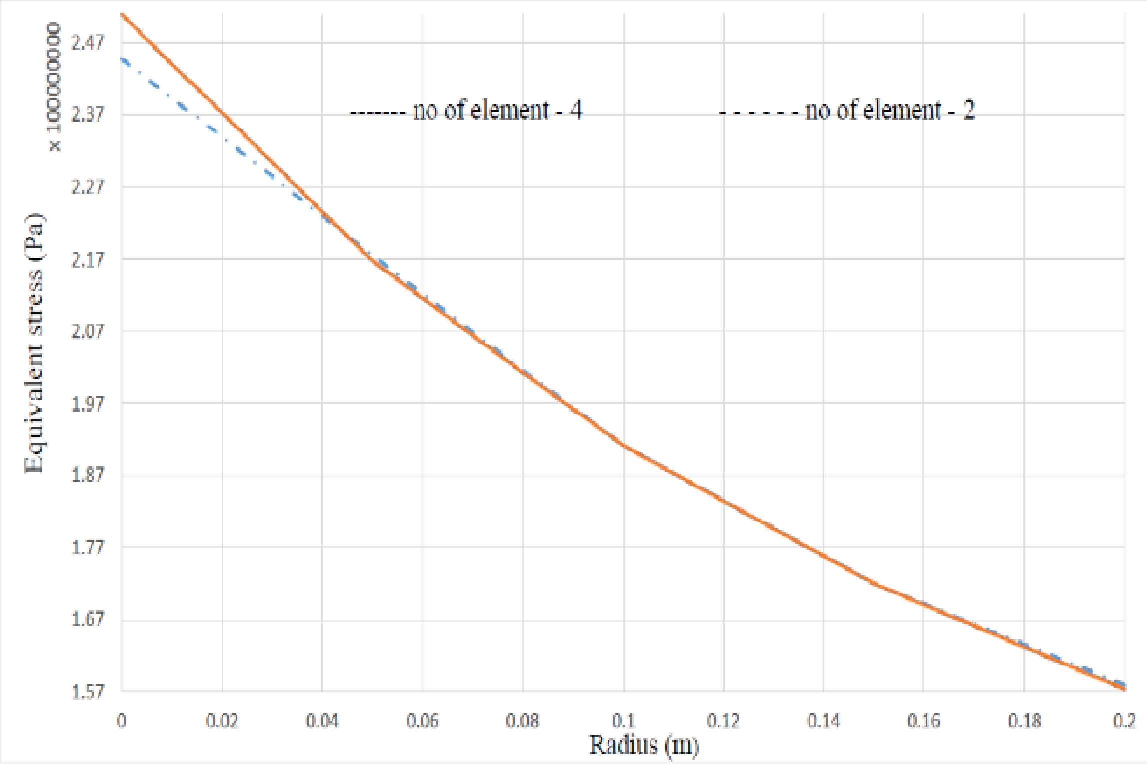

Fig 16: equivalent stress vs radius (ω = 50rad /sec)

.

6.4. Discussions:

By this far, all the equations have been formulated that are required for the further analysis to be done. At first the general stress equilibrium equation for an axisymmetric structure is taken and with the assumed boundary conditions, the values of constants are evaluated. Then the Kirchhoff's law of steady state heat conduction is added to the general equation of stress and the values of new set of constants are evaluated. Now that all the required equations for analytical analysis is done, some case studies are taken for further analysis.

By taking a case study, the validation of the procedure being followed for the ongoing research is established. The above being done in simulation software, the next step will be to do the same analytically.

For special case, temperature gradient is introduced in the structure for further analysis. The results so obtained are shown in the graphs above.

During mathematical evaluation for the expression of displacement function, stress due to inside pressure, thermal gradient has been taken into account. Since it is assumed that the material of the structure is isotropic & homogeneous, the elastic modulus, thermal coefficient of heat conduction, density & linear coefficient of expansion have been considered to be unvarying with radius.

From analysis, it has come to notice that the radial deformation & stress components in the cylinder under thermal load in different directions increases substantially. Hence the performance of an axisymmetric cylinder under thermal environment degrades.

By comparing the results obtained from ANSYS- Structural, the results obtained from mathematical analysis using FEM by MATLAB are found to be in close in value.

Chapter 7

Conclusion

By subjecting the axisymmetric cylinder to the thermal gradient load, it is found that the stress components and deformation values increases substantially.

Mathematical analysis on MATLAB using FEM method shows that by increasing the no of element, the stress values & displacement function values approach the result obtained from ANSYS-Structural analysis. Hence the convergence test succeeds.

Since the temperature term is included in the expression of the displacement expression, it is worthwhile to see the effects of temperature gradient on the displacement function and stress components.

[1]Paul E. Lyon Axisymmetric finite element modeling for the design and analysis of cylindrical adhesive joints based on dimensional stability J. Bas. Eng. 87 (2010) 877

[2]M. Zamani Nejad and G. H. Rahimi*, 2010, "Elastic analysis of FGM rotating cylindrical pressure vessels",Scientific Research and Essay Vol.4 (3), pp. 131-140, March, 2010.

[3]H.R.Eipakchi; S.E.Khadem; and G.H. Rahimi S., 2008, "Axisymmetric Stress Analysis of a thick conical shell with varying thickness under non-uniform internal pressure." Journal of Engineering Mechanics, Vol.134, No.8, August1, 2008. ©ASCE, ISSN 0733- 9399/2008/8-601ñ610.

[4]George F. HAUSENBAUER ** and George C. LEE, 1966, "Stresses in ThickWalled Conical Shells". NUCLEAR ENGINEERING AND DESIGN 3 ¢1966) 394- 401.

[5]S.A.Tavares, 1995, "Thin Conical shells with constant thickness and under axisymmetric load".Computers and Structures Vol 60, No 6. pp 895-921. 1996.

[6]S. Taira et al., Creep of thick walled cylinders under internal pressure at elevated temperature, Proc. 8th Japan Congress on Test. Mat., Soc. Mat. Sci., Kyoto, Japan 53 (1965).

[7]N.S. Bhatnagar, P.S. Kulkarni and V.K. Arya, 1984, "Creep Analysis of an internally pressurized orthotropic rotating cylinder" Nuclear Engineering and Design 83 (1984) 379-388.

[8]Renton, J.W., and Vinson, J.R, 1975, "The Efficient Design of Adhesive Bonded Joints," J. Adhesion, 7, pp. 175-193.

[9]Renton, J.W., and Vinson, J.R., 1975, "On the Behavior of Bonded Joints in Composite Material Structures," Engineering Fracture Mechanics, 7, pp. 41-60.

[10]Potter, K.D., Guild, F.J., Harvey, H.J., Wisnom, M.R., and Adams, R.D., 2001, "Understanding and Control af Adhesive Crack Propagation in Bonded Joints Between Carbon Fibre Composite Adherends – I. Experimental," Int. J. Adhesion and Adhesives, 21, pp. 435-443.

[11]F.P.J.Rimrott, Creep pf thick walled tubes under internal pressure considering large strains, J. Materials Science, 39, pp. 4729-4797.

[12]A. Nadai, “On the creep of Solids at elevated temperatures”, Journal of Applied Physics, Vol. 8, 1937, pp. 418-446

[13]Anderson, G. P., DeVries, K. L., and Sharon, G., 1982, “Evaluation of Adhesive Test Methods,” Adhesive Joints: Formation, Characteristics, and Testing, Plenum Press, New York, pp. 269-288.

[14] Shimoda, T., He, J., and Aso, S., 2006, “Study of Cryogenic Mechanical Strength and Fracture Behavior of Adhesives for CFRP Tanks of Reusable Launch Vehicles,” 1, Memoirs of the Faculty of Engineering, Kyushu University, 66, pp. 55-70.

[15] Potter, K.D., Guild, F.J., Harvey, H.J., Wisnom, M.R., and Adams, R.D., 2001, “Understanding and Control af Adhesive Crack Propagation in Bonded Joints Between Carbon Fibre Composite Adherends – I. Experimental,” Int. J. Adhesion and Adhesives, 21, pp. 435-443.

[16] Graf, N.A., Schieleit, G. F., and Biggs, R., “Adhesive Bonding Characterization of Composite Joints for Cryogenic Use,” NASA Report Number NCC8-116, NASA Technical Reports Server.

[17] Nemes, O., Lachuad, F., and Mojtabi, A., 2007, “Contribution to the Study of Cylindrical Adhesive Joining,” Int. J. Adhesion and Adhesives, 26, pp. 474-480.

[18] Shi, Y.P., and Cheng, S., 1993, “Analysis of Adhesive-Bonded Cylindrical Lap Joints Subjected to Axial Load,” J. Engineering Mechanics, 119, pp. 584-602.